American Journal of Case Reports

e-ISSN 1941-5923
© Am J Case Rep, 2026; 27: e952355
DOI: 10.12659/AJCR.952355

Received: 2025.12.07
Accepted: 2026.04.29
Available online: 2026.05.07
Published: 2026.XX.XX

Depicting Characteristic Staghorn Vessels in Solitary Fibrous Tumor of the Liver With Contrast-Enhanced Ultrasound and Ultrasound Localized Microscopy: A Case Report

Authors' Contribution:
Study Design A
Data Collection B
Statistical Analysis C
Data Interpretation D
Manuscript Preparation E
Literature Search F
Funds Collection G

ABCDEFG 1 Xue Lu
BCDE 2 Yuanqiang Xiao
BCD 1 Lili Wu
BCD 3 Jianning Chen
BF 1,4 An Liu
CDFG 1 Jie Ren
AEFG 1 Yinglin Long

1 Department of Ultrasound, The Third Affiliated Hospital of Sun Yat-Sen University, Guangzhou, Guangdong, PR China
2 Department of Radiology, The Third Affiliated Hospital of Sun Yat-Sen University, Guangzhou, Guangdong, PR China
3 Department of Pathology, The Third Affiliated Hospital of Sun Yat-Sen University, Guangzhou, Guangdong, PR China
4 Department of Ultrasound, Fengshun County People's Hospital, Meizhou, Guangdong, PR China

Corresponding Authors: Yinglin Long, e-mail: longylin3@mail.sysu.edu.cn, Jie Ren, e-mail: renjieguangzhou@126.com
Financial support: The work is supported by the National Natural Science Foundation of China under grant No.82302221; The Third Affiliated Hospital of Sun Yat-Sen University, Clinical Research Program No. QHJH202302; National Natural Science Foundation Cultivation Project No. 2023GZRPYQN06; and Guangzhou Science and Technology Plan Project under grant No: 2023A03J0728

Conflict of interest: None declared

Patient: Female, 55-year-old

Final Diagnosis: Solitary fibrous tumor of the liver

Symptoms: Asymptomatic

Clinical Procedure: —

Specialty: Gastroenterology and Hepatology

Objective: Rare disease

Background: Solitary fibrous tumor of the liver (SFTL) is a rare mesenchymal neoplasm. Most patients are asymptomatic, and lesions are discovered accidentally. Lacking specific imaging manifestations, SFTL is prone to misdiagnosis, making accurate preoperative diagnosis vital for clinical treatment. Thus, multimodal imaging is indispensable for preoperative evaluation.

Case Report: We report the case of a 55-year-old woman with an asymptomatic liver mass identified during a routine health examination. Initial contrast-enhanced ultrasound (CEUS) revealed a hypervascular lesion with abundant peripheral blood flow and distinct intratumoral tortuous vascular signals. To further characterize these findings, ultrasound localized microscopy (ULM) was employed. This advanced imaging technique vividly delineated the characteristic "staghorn-shaped" branching vessels within the tumor, providing a pivotal preoperative clue highly suggestive of SFTL. Preoperative multi-modality imaging demonstrated that the tumor was hypervascular and located adjacent to the inferior vena cava, making direct resection highly risky. In view of its hypervascularity and unfavorable anatomical location, neoadjuvant transarterial chemoembolization (TACE) was performed preoperatively to reduce tumor volume. This downsizing successfully transformed a potentially high-risk resection into a feasible procedure, enabling a subsequent safe and margin-negative surgical resection. Histopathological examination of the resected specimen confirmed the diagnosis of SFTL and corroborated the presence of the characteristic staghorn vascular pattern observed on imaging.

Conclusions: In conclusion, combined CEUS and ULM effectively displays characteristic vascular signs of SFTL to assist differential diagnosis. Preoperative TACE is an effective neoadjuvant approach for anatomically difficult SFTL to facilitate radical surgery. Further large-sample long-term follow-up studies are needed to verify the conclusions, due to limited single-case data.

Keywords: Chemoembolization, Therapeutic • Liver Neoplasms • Solitary Fibrous Tumors • Ultrasonography, Doppler, Color • Radiology • Contrast Media • Ultrasonography • Chemoembolization, Therapeutic • Case Reports

Full-text PDF: https://www.amjcaserep.com/abstract/index/idArt/952355

2526 2 6 23

Indexed in: [PMC] [PubMed] [Emerging Sources Citation Index (ESCI)] [Web of Science by Clarivate]

Introduction

Solitary fibrous tumor of the liver (SFTL) is an exceptionally rare tumor originating from fibroblastic mesenchymal tissues, comprising spindle cells and collagen [1]. The tumors are most commonly seen in middle-aged individuals, with no obvious sex predilection reported in the limited existing literature [2]. Meanwhile, SFTLs are asymptomatic and identified incidentally and are detected during routine physical examinations in the previous cases [2,3].

Although previous studies reported the B-ultrasound, magnetic resonance imaging (MRI), and contrast-enhanced ultrasound (CEUS) findings of SFTL, these findings lack specificity. In addition, most case reports describe only a single imaging modality, with a lack of reports on the multi-modality imaging characteristics in the same case [4,5]. An additional constraint is that most case reports are confined to a single imaging modality, with limited literature documenting multi-modality characteristics in the same patient [4,5].While definitive diagnosis ultimately relies on histopathology, which reveals characteristic structures such as staghorn vessels, these thin vascular channels are too delicate to be clearly visualized on routine imaging modalities including computed tomography (CT), MRI, and CEUS. This combination of nonspecific imaging findings and limited multi modality data creates substantial challenges for accurate preoperative differential diagnosis from hepatocellular carcinoma (HCC), fibrolamellar HCC, and metastatic lesions [6].

Radical surgical resection with negative margins has been performed in previous cases of SFTL in which the tumor was confined to the liver and distant from major hepatic vessels [1]. However, when the tumor is adjacent to major hepatic vessels, direct primary resection carries high surgical risk and technical difficulty. Multi-modality imaging aids tumor characterization, provides pathological clues, and precisely delineates tumor-vessel relationships. Thus, preoperative imaging is critical for individualized treatment and risk reduction. Without reliable imaging, misdiagnosis is common, leading to delayed or overtreatment.

Ultrasound localized microscopy (ULM) is an advanced imaging modality built on the foundation of CEUS. By precisely identifying individual microbubble contrast agents and dynamically tracking their spatial displacements in serial CEUS image sequences [7], ULM achieves a high spatial resolution down to the tens of micrometers scale [8], thus allowing for the highly detailed networks of microvasculature. Zheng et al reported that ULM can visualize the morphological characteristics of microvasculature within breast lesions, which confers important diagnostic value for the differentiation of benign and malignant breast lesions [9]. However, the application of ULM in SFTL has been rarely reported to date.

This case report presents the microvascular characteristics of SFTL visualized by ULM, together with its multimodality imaging findings and treatment strategy. It provides new insights for the diagnosis and optimized treatment of SFTL.

Case Report

A 55-year-old female patient was incidentally found to have a liver mass on a chest CT performed as part of routine health screening, without abdominal pain. The patient had no systemic symptoms (weight loss, fatigue, or anorexia) or relevant risk factors (alcohol use and metabolic syndrome). Physical examination revealed no positive findings. Tumor markers, including CEA, AFP, FER, CA125, CA19-9, CA15-3, were tested, and none were elevated. The patient had no history of chronic liver disease or hepatitis B infection, and her liver function panel (aminotransferase levels, bilirubin, albumin, and international normalized ratio) was within the reference range (**Table 1**).

An abdominal ultrasound examination was conducted, which revealed a hepatic space-occupying lesion with undetermined pathological nature. It revealed an oval mass measuring approximately 58 × 48 mm in segments I/II/IV. The lesion demonstrated mixed echogenicity with heterogeneous internal echoes and scattered hyperechoic foci. Color Doppler imaging showed abundant intralesional and peripheral vascularity. The mass was observed to displace and compress the left portal vein and left hepatic vein, resulting in the loss of clear boundaries between the vessels and the tumor.

CEUS was subsequently performed to characterize the vascular perfusion patterns of the lesion. SonoVue contrast (1.5 mL) was administered through the antecubital vein, and CEUS images were obtained on a Mindray Resona A20 ultrasound unit for 2 minutes. The main mass exhibited hyperenhancement in the arterial phase, which progressed to hypoenhancement in the portal venous and delayed phases (**Figure 1**). Tortuous intratumoral microvessels and peripheral annular vessels were visualized during the arterial phase. This enhancement pattern definitively ruled out focal nodular hyperplasia (FNH) and hepatic metastases, narrowing the differential diagnosis spectrum. However, some features on CEUS and MRI, such as contrast washout and incomplete capsular enhancement, were highly similar to those of HCC, which increased the difficulty of differential diagnosis.

To further depict the vascular characteristics of the tumor, ULM was performed to generate a microscopic blood flow map during the arterial phase. ULM was conducted by a radiologist with over 5 years of abdominal ultrasound experience using a Mindray Resona A20 ultrasound system (Mindray Bio-Medical Electronics Co, Ltd, Shenzhen, China) equipped with a C6-1 linear probe (1-6 MHz) in adult abdominal mode, with

Indexed in: [PMC] [PubMed] [Emerging Sources Citation Index (ESCI)] [Web of Science by Clarivate]

Table 1. The serological results of the patients.

Test name	Result	Unit	Reference range
CEA	2.56	μg/L	0-5.0 μg/L
AFP	1.02	ng/mL	0-8.1 ng/mL
FER	246.87	ng/mL	10-291 ng/mL
CA19-9	16.08	U/mL	0-35 U/mL
CA125	13.00	U/mL	0-35 U/mL
CA15-3	8.80	U/mL	0-35 U/mL
ALT	22	U/L	13-35 U/L
AST	21	U/L	3-35 U/L
Total bilirubin	7.9	mmol/L	4.0-23.9 μmol/L
Direct bilirubin	1.6	mmol/L	0.0-6.8 μmol/L
Indirect bilirubin	6.3	mmol/L	2.6-20.9 μmol/L
INR	0.92	–	0.8-1.5
Albumin	34.6	g/L	35-50 g/L

CEA, carcinoembryonic antigen; AFP, alpha-fetoprotein; FER, serum ferritin; CA199, carbohydrate antigen 19-9; CA125, carbohydrate antigen 125; CA153, carbohydrate antigen 15-3; ALT, alanine aminotransferase; AST, aspartate aminotransferase; INR, international normalized ratio.

scanning depth set at 15 cm, mechanical index at 0.110, and frame rate ≥300 fps. Before examination, patients received breathing training to maintain steady respiration and 3 to 5 seconds of breath-holding to reduce respiratory artifacts and were placed in a supine position with arms abducted to fully expose the target area, which was horizontally aligned using soft pads. An additional 1.5 mL of SonoVue contrast agent was intravenously injected via the antecubital vein as a bolus, followed by a 5-mL normal saline flush. Dynamic ULM imaging was initiated immediately after injection, with data acquired specifically in the arterial phase (20 seconds after injection, corresponding to peak contrast enhancement), and raw data were continuously acquired for no less than 60 seconds and stored for subsequent analysis.

The ULM demonstration revealed relatively abundant blood flow signals inside and around the mass. Furthermore, it confirmed abundant microvasculature within the tumor. A circumferential blood flow pattern was observed around the tumor periphery, and multiple branching microvessels inside the lesion, some exhibiting double bifurcations, presented a morphology staghornshaped vascular (**Figure 1**). This distinctive vascular feature provided crucial evidentiary support for the definitive diagnosis of SFTL.

Contrast-enhanced MRI was performed. A well-defined mass (54×48×56 mm) in segments I/II/IV demonstrated hypointensity on T1-weighted imaging and hyperintensity on T2-weighted imaging. Dynamic contrast-enhanced MRI revealed marked heterogeneous enhancement in the arterial phase, followed by washout in most regions during portal venous and delayed phases, with partial persistent enhancement. An incomplete peripheral capsular enhancement was noted (**Figure 2**).

The tumor's proximity to the inferior vena cava meant that direct surgical resection carried substantial technical challenges and risks. Given the non-standard nature of transarterial chemoembolization (TACE) for SFTL, the treatment strategy was determined through multidisciplinary discussion and informed consent, with TACE recommended as initial treatment in view of the tumor's hypervascular nature in the arterial phase rendering this approach feasible. Under digital subtraction angiography guidance, the patient underwent right femoral artery puncture under local anesthesia, with a 4F P-RH catheter advanced into the celiac artery. Angiography revealed tortuous, disordered hepatic vessels and ill-defined tumor staining, and a microcatheter was selectively inserted into the tumor-feeding branch of the left hepatic artery to perform treatment with a mixture of 5 mL Lipiodol and 1 vial of pingyangmycin, followed by Embosphere microspheres. Post-procedural angiography showed significantly diminished tumor staining without contrast extravasation. After catheter removal and puncture site hemostasis, the patient was transferred to the ward.

Indexed in: [PMC] [PubMed] [Emerging Sources Citation Index (ESCI)] [Web of Science by Clarivate]

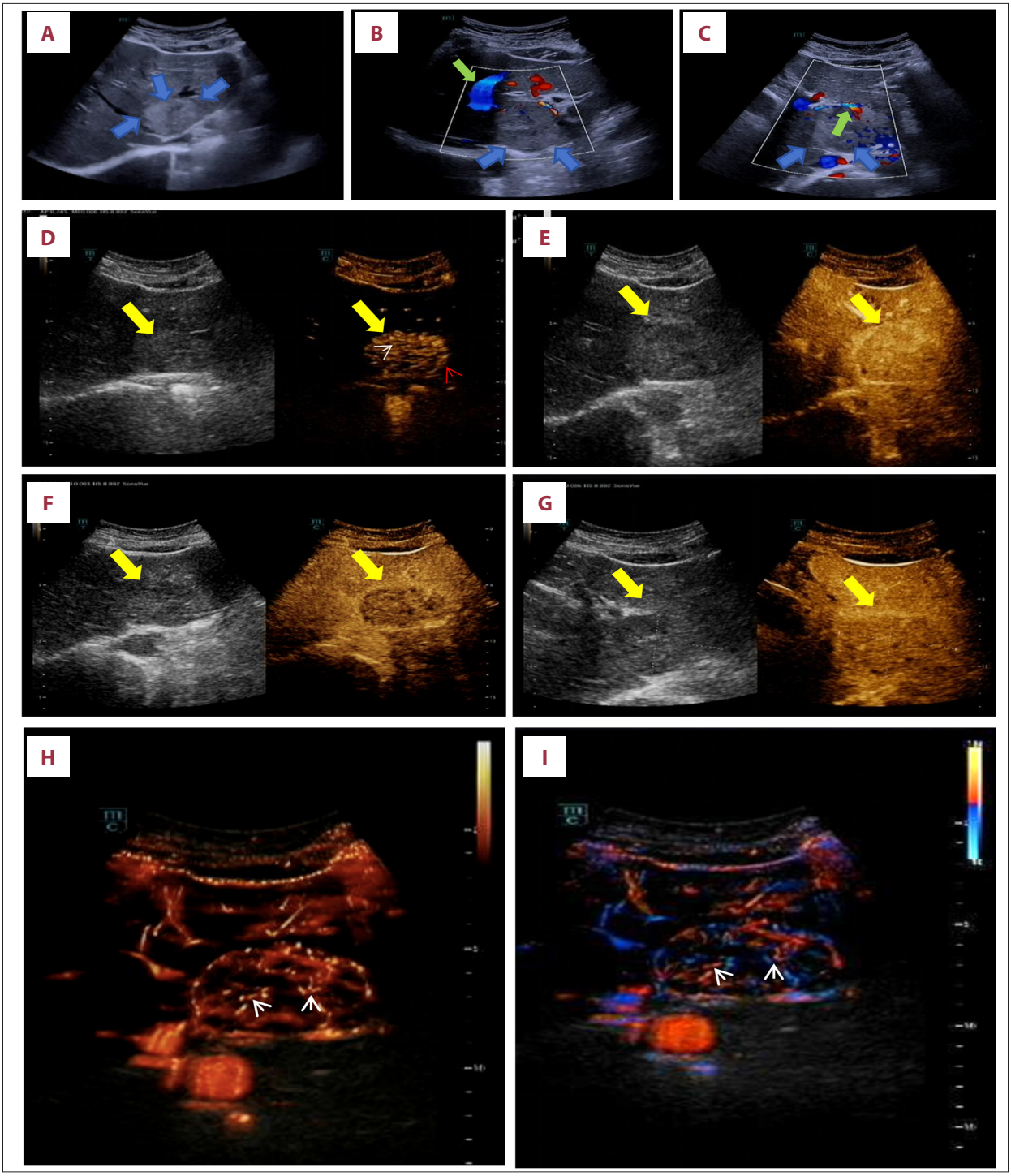

Figure 1. B-mode ultrasound, contract-enhanced ultrasound and ultrasound localized microscopy (ULM) imaging. (**A**) B-mode ultrasound shows an oval mass (blue arrow) in segment II. (**B, C**) On color Doppler flow imaging, peripheral vessels (green arrow) are seen around the mass (yellow circle), with no significant internal vascularity. (**D-G**) Contrast-enhanced ultrasound (CEUS) images of the mass. (**D-F**) images correspond to the early arterial phase (11 s), late arterial phase (22 s), portal phase (50 s), and delayed phase (139 s), respectively. The lesion shows arterial phase hyperenhancement followed by hypoenhancement in the portal and delayed phases. In the arterial phase (**D**), tortuous microvessels within the tumor (white arrow) and surrounding annular vessels (red arrow) are visible. (**H, I**) ULM images demonstrate characteristic staghorn-shaped vessels within the lesion (white arrow). (**H**) Blood flow velocity map; (**I**) blood flow direction map.

Indexed in: [PMC] [PubMed] [Emerging Sources Citation Index (ESCI)] [Web of Science by Clarivate]

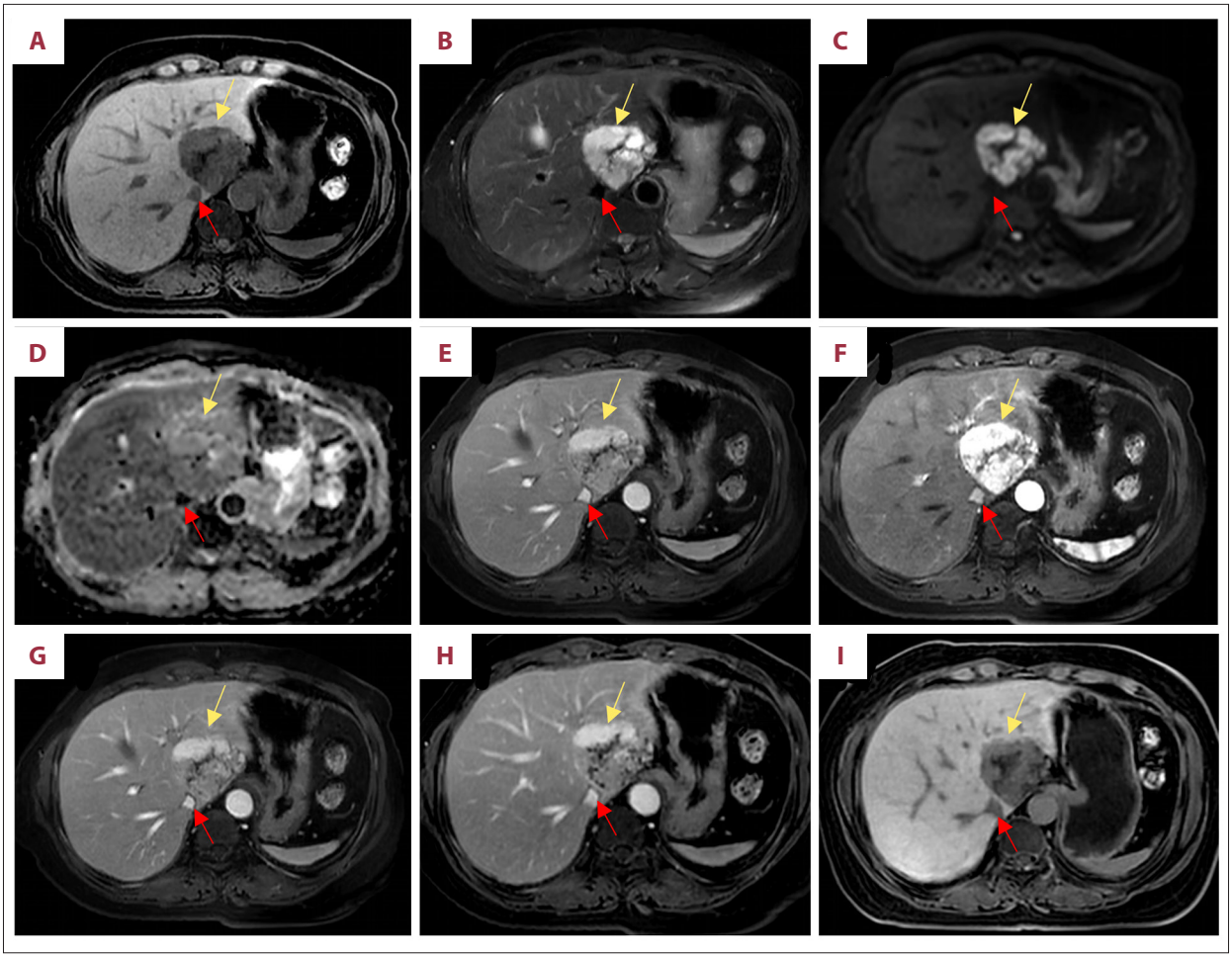

Figure 2. A 55-year-old woman with pathologically confirmed solitary fibrous tumor (orange arrow) in the liver, which is closely adjacent to the inferior vena cava (the red arrow). Preoperative MR examination suggests the tumor shows (**A**) hypointensity on T1-weighted imaging, (**B**) hyperintensity on fat-suppressed T2-weighted imaging, (**C**) exhibits restriction on diffusion-weighted imaging (b=800), and (**D**) apparent diffusion coefficient images. Dynamic contrast-enhanced MRI reveals that (**E**) the lesion with arterial phase hyperenhancement followed by (**F**) washout in the portal phase. (**F-H**) Persistent peripheral rim enhancement is noted in the portal, venous, and delayed phases. (**I**) On hepatobiliary phase imaging, the lesion is hypointense compared with the background liver parenchyma and contains an internally hypointense scar.

In the meanwhile, liver biopsy was performed during TACE (**Figure 3**). Liver biopsy showed absent normal hepatic architecture, spindle-shaped atypical tumor cells, intracytoplasmic pigment, and stromal collagenization, highly suggestive of SFTL, with definitive subtype pending surgical specimen. Immunohistochemistry results showed CD34 (+), ERG (-), SOX10 (-), CK (-), Vimentin (+), Ki-67 (5%+), HMB45 (-), Melan-A (-), S100 (-), H3K27Me3 (+, no loss), DOG-1 (-), CD117 (-), STAT6 (+). Special staining showed iron staining (-) and reticulin staining (+, fibrous stromal tissue).

CT and MRI at 2 months after TACE treatment demonstrated that the tumor regressed to 41×36 mm, representing a volume reduction of 47% and making the complete surgical resection feasible (**Figures 4, 5**).

Then, the patient underwent left hemihepatectomy with caudate lobectomy and cholecystectomy. Histopathological examination revealed a tumor composed of short spindle or ovoid cells with scant cytoplasm and nuclear atypia, accompanied by collagenized stroma and characteristic staghorn-shaped vessels. Focal degenerative cellular changes and extensive necrosis were also observed. Immunohistochemistry showed positivity for CD34 and STAT6, findings consistent with a solitary fibrous tumor with post-embolization changes (**Figure 6**).

The patient was followed up at 1, 3, and 6 months postoperatively. No symptom was reported, and no signs of tumor recurrence were evident on imaging studies. Tumor markers also remained within normal limits. Beyond imaging and tumor markers, the patient's postoperative recovery was uneventful.

Indexed in: [PMC] [PubMed] [Emerging Sources Citation Index (ESCI)] [Web of Science by Clarivate]

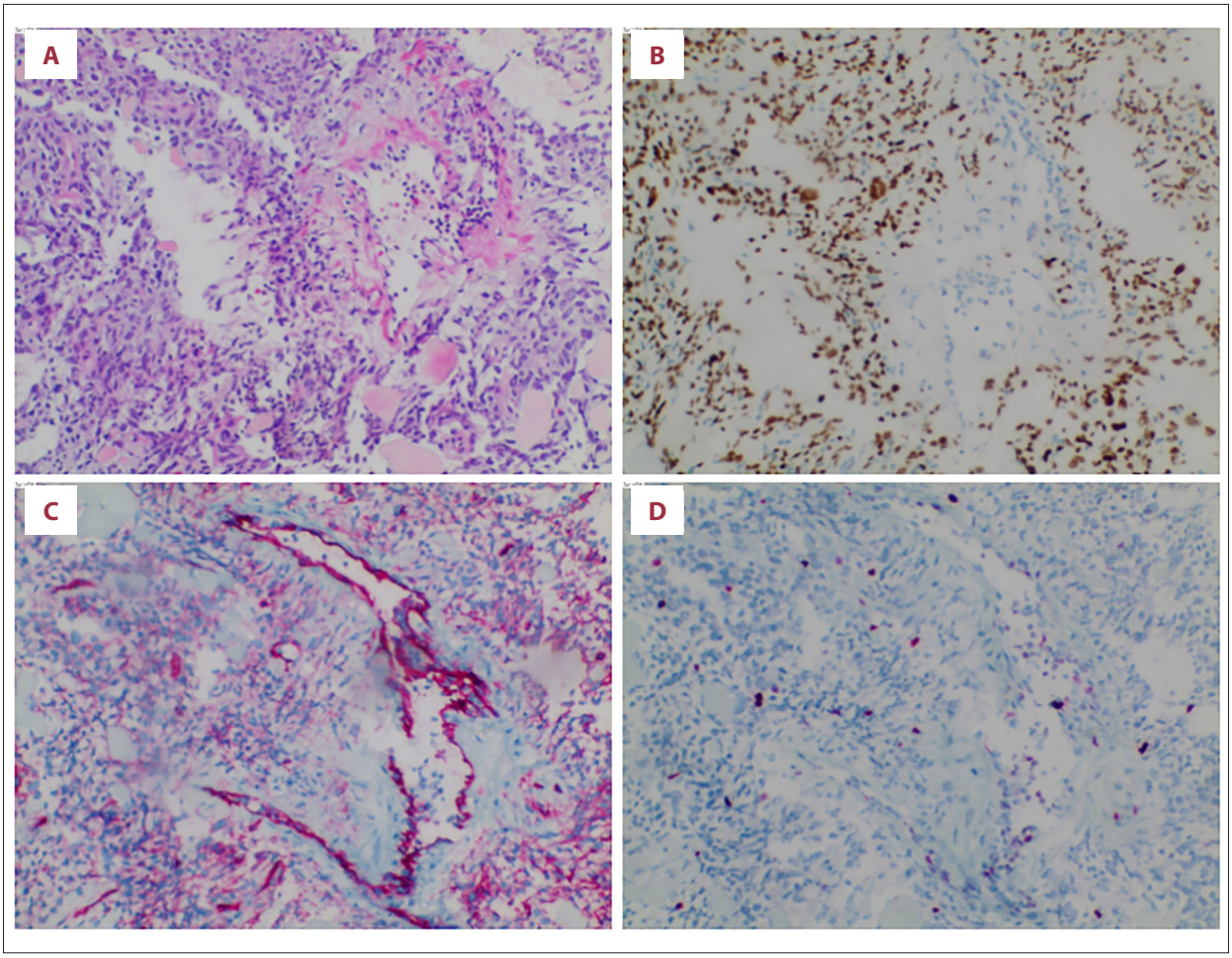

Figure 3. Pathological features of the punctured tissue. (**A**) Hematoxylin and eosin staining (×100) shows loss of the normal fascicular architecture. Tumor cells are spindle-shaped and arranged in fascicular or disorganized patterns, with cellular atypia and rare mitotic figures. Intracytoplasmic pigment is present in some cells, and stromal collagenization is observed. (**B-D**) Immunohistochemical staining (100×) demonstrates positive expression of STAT6 (**B**), CD34 (**C**) and Ki-67 (5% positive, **D**), respectively.

She was completely free of pain, had no limitation in physical activity, and required no readmission during 6 months of follow-up.

Discussion

Previous cases have reported the imaging findings of SFTL, and most have focused on CT and MRI characteristics. SFTL often present as a heterogeneously enhancing mass in CT images [1-3,5]. On MRI, it appears hypointense on T1-weighted images and hyperintense on T2-weighted images. Only 1 case reported the findings of CEUS [4]. The described CEUS features [4], which encompass peripheral arterial enhancement with rapid centripetal filling, peak-phase heterogeneity, and subsequent wash-out, were present in our case as well. However, these characteristics are not characteristic and are shared by many other liver tumors.

To the best of our knowledge, ULM has rarely been reported to visualize the intratumoral microvasculature of a solitary fibrous tumor. ULM is an advanced ultrasound technique that enables microvascular depiction at a resolution finer than the hundreds-of-microns scale [10]. While CEUS revealed tortuous vessels within the tumor, ULM delineated these subtle structures with far greater clarity, demonstrating staghornshaped vascular patterns in some areas. Furthermore, real-time CEUS during the arterial phase identified not only tortuous microvessels inside the tumor but also surrounding annular vessels.

These detailed imaging characteristics closely correspond to the underlying pathological features of the lesion. Histologically, SFTL is characterized by spindle to ovoid cells exhibiting a

Indexed in: [PMC] [PubMed] [Emerging Sources Citation Index (ESCI)] [Web of Science by Clarivate]

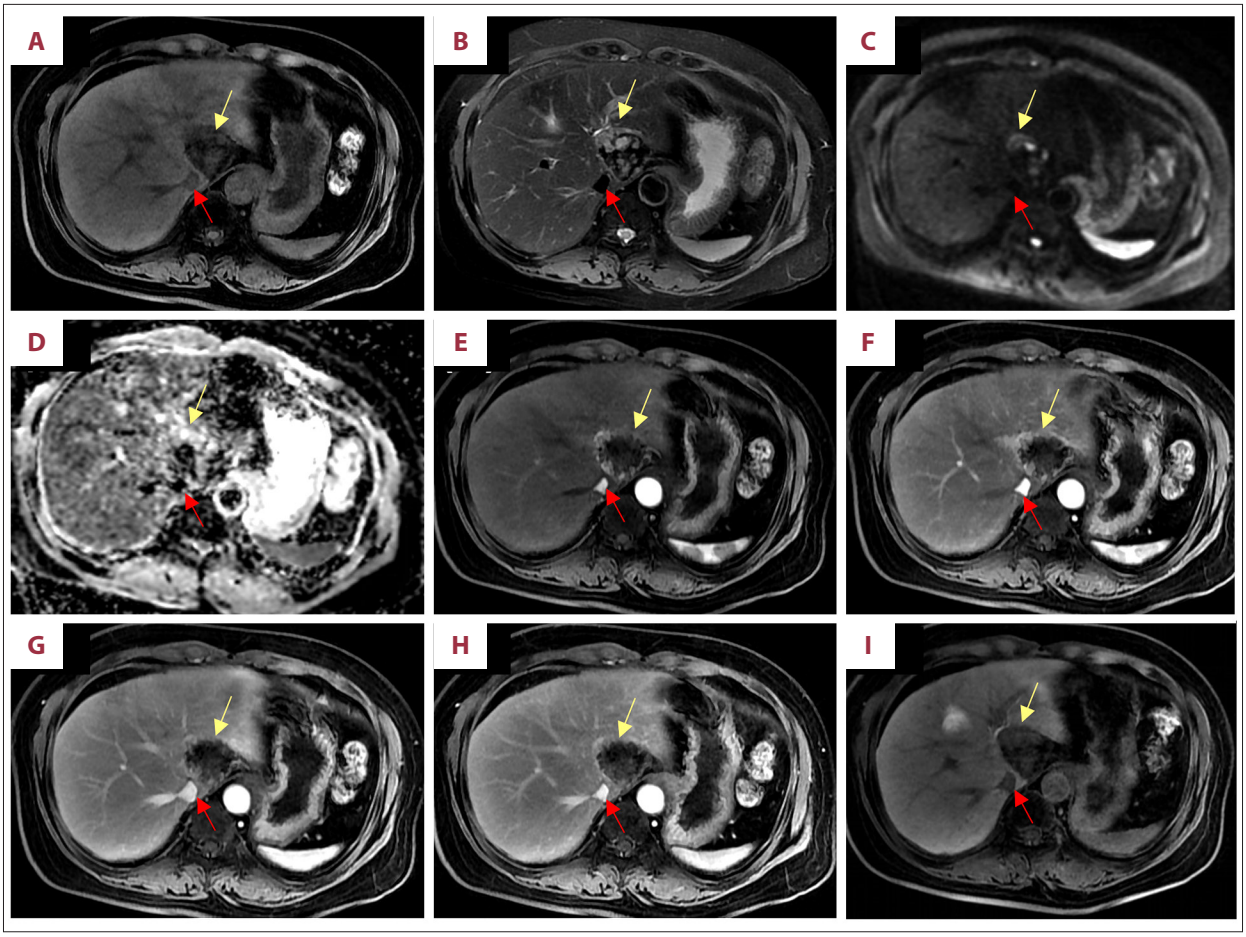

Figure 4. After 2 sessions of transarterial chemoembolization (TACE), MRI shows the following findings. (**A**) T1-weighted imaging demonstrates mixed hypointensity of the tumor (orange arrow). (**B**) Fat-suppressed T2-weighted imaging shows mixed hyperintensity. (**C, D**) Diffusion-weighted imaging (b=800 s/mm^2) and corresponding apparent diffusion coefficient images demonstrate partial restricted diffusion. (**E-H**) Dynamic contrast-enhanced MRI shows minimal delayed peripheral enhancement, with a marked reduction in the enhancing area compared with prior imaging. (**I**) On hepatobiliary phase imaging, the lesion is hypointense relative to the background liver parenchyma, with focal isointense areas at the tumor margins. The tumor (orange arrow) is clearly demarcated from the inferior vena cava (red arrow).

predominantly patternless growth, with abundant collagen in the stroma. This typically presents as a hyperechoic nodule on 2dimensional ultrasound. Classic histological features include fascicles of spindle cells arranged in a fibrous stroma, along with the characteristic staghorn-like vascular pattern. This vasculature is characterized by thin-walled, branching vessels which serve as a crucial diagnostic clue for SFTL [11]. Notably, this vascular architecture can be directly visualized as a staghornlike pattern on ULM.

The enhancement pattern and vascular features identified via CEUS and ULM are critical for differentiating SFTL from well-differentiated HCC, FNH, and angiomyolipoma (AML). The systematic comparison between these 4 tumors is presented in **Table 2** [1,4-6,12-18]. Key imaging findings that support the diagnosis of SFTL include intrinsic and extensive intratumoral small-vessel proliferation, which is demonstrated by ULM/CEUS as characteristic staghorn vessels characterized by regular, tree-like branching without disorganization or cross-linking, along with arterial phase hyperenhancement driven by this intrinsic vascular network. Unlike HCC, which relies on external, disorganized feeding vessels (penetrating, tortuous, cross-linked) to expand arterial supply and shows characteristic delayed-phase washout [19], the current lesion lacked external feeding vessels and delayed washout. Hence, HCC was ruled out. For a female patient without hepatitis B infection, a lesion showing arterial phase hyperenhancement with washout requires differentiation of FNH [20]. However, in this case, the characteristic central scar and spoke-wheel enhancement of FNH were not observed, making FNH a less likely diagnosis. Patchy hyperechoic areas suggested the presence of fatty components, which is one of the key imaging features of

Indexed in: [PMC] [PubMed] [Emerging Sources Citation Index (ESCI)] [Web of Science by Clarivate]

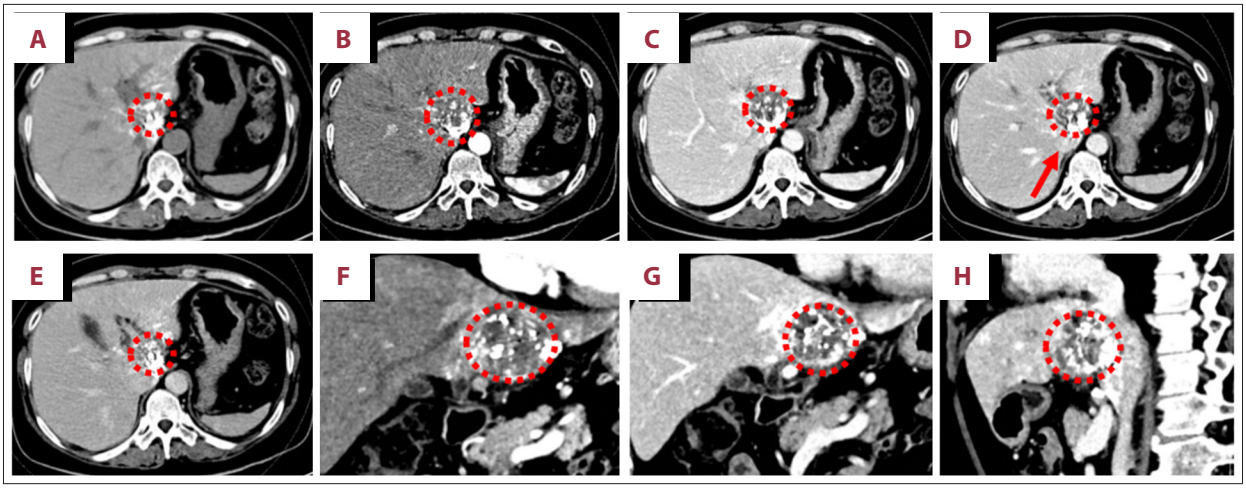

Figure 5. After 2 sessions of transarterial chemoembolization (TACE) treatment, (**A**) computed tomography findings suggest the tumor (red dotted circle) shows mixed density on non-enhanced image, which iodine oil scattered deposition within the lesion, mainly at the edge of the lesion. (**B-H**) The lesion shows uneven enhancement on the enhanced image, and the edge shows incomplete enhancement capsule, with a significant reduction in the enhanced area compared with before TACE images. (**D**) The main tumor (red dotted circle) is clearly demarcated from the inferior vena cava (red arrow).

AML. However, blood vessels in AML typically show a tortuous course, with heterogeneous enhancement observed within the tumor. In this case, the presence of fatty components and heterogeneous enhancement did not allow complete exclusion of AML. Nevertheless, the tumor vessels showed a distinct staghorn-like pattern, so AML was not regarded as the primary diagnostic consideration.

Our case also provides multi-modality imaging in 1 patient. Imaging modalities complemented each other in guiding treatment. CEUS clarified vascular details, CT defined spatial relationships for surgical planning, and MRI characterized tissue components (fat, fluid, soft tissue). Their integrated findings ensured accurate evaluation and optimized decisionmaking.

Complete surgical resection with negative margins remains the gold standard treatment for localized disease [1]. However, there is currently no established consensus regarding the management of SFTL adjacent to critical hepatic vascular structures in which surgical risks are prohibitively high. Given that SFTL is a hypervascular neoplasm whose growth and metastatic dissemination are fundamentally angiogenesis-dependent [21], the tumor in this case was large in volume and located adjacent to major intrahepatic vessels, resulting in an excessively high risk of intraoperative hemorrhage if direct surgical resection were performed. Therefore, TACE performed before surgery can reduce the risk of intraoperative bleeding by embolizing the tumor's blood supply arteries; meanwhile, it can shrink the tumor size through local effects to improve the feasibility of surgical resection for larger or complex liver tumors[1,22,23]. Thus, preoperative TACE was performed. TACE successfully achieved significant tumor volume reduction, thereby facilitating subsequent curative resection. Hence, TACE may be considered in selected cases in which complete surgical resection is technically challenging. In our case, left lobectomy with caudate lobectomy was chosen over limited enucleation for hepatic SFTL. Dorsal location far from the hepatic capsule made enucleation technically difficult with incomplete resection risks, and preoperative biopsy only confirmed the diagnosis but lacked sufficient histological data to assess malignant potential due to limited sampling. Meanwhile, since the tumor involved hepatic segments I/II/IV and was adjacent to the gallbladder, cholecystectomy was also required. Therefore, radical resection was performed to avoid residual lesions in accordance with clinical principles.

Despite the encouraging findings, this study has several limitations. First, although our study reported that ULM can reveal the characteristic staghorn-shaped blood vessels in SFTL, the novelty of ULM should be tempered by noting the lack of comparative validation. Second, this is a case report, which inherently limits the generalizability of the results. Due to the low incidence of this disease, our findings will need to be validated in a larger number of future cases. Third, the follow-up period was only 6 months, which may not be sufficient to fully assess long-term outcomes, highlighting the need for extended monitoring in future research.

Conclusions

SFTL is a rare tumor. The multimodal imaging features were presented in this case, in which CEUS and ULM revealed tortuous vessels within the lesion, potentially offering a clue for

Indexed in: [PMC] [PubMed] [Emerging Sources Citation Index (ESCI)] [Web of Science by Clarivate]

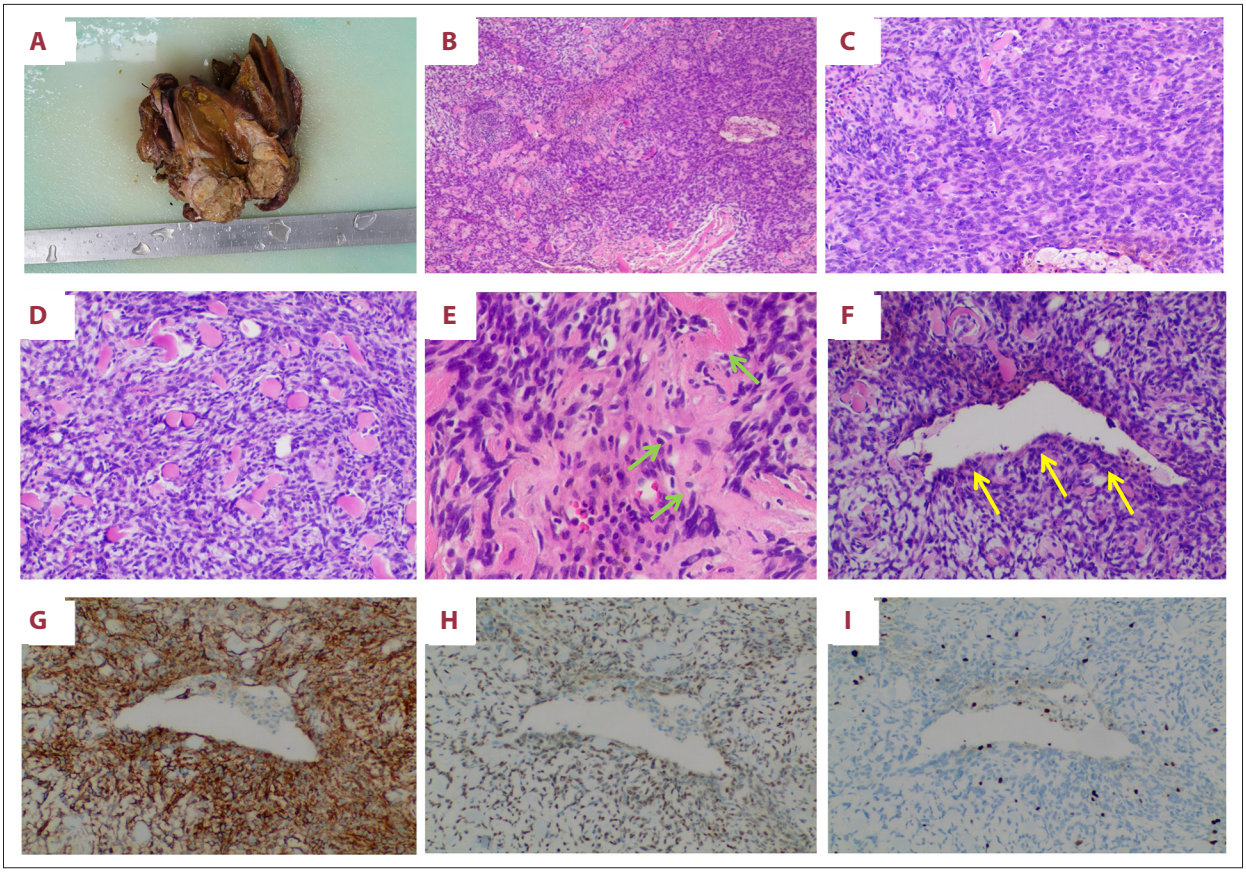

Figure 6. The histological features are consistent with the presentation of hepatic solitary fibrous tumor. (**A**) The resected specimen. (**B-F**) Microscopic pathology. The tumor cells are short spindle-shaped or oval, arranged diffusely or in bundles (**B**), with areas showing higher cellular density (**C**) and others with lower cellular density (**D**). Abundant coarse collagen bundles (green arrow) are observed in the stroma (**E**). Characteristic "staghorn-shaped" blood vessels (yellow arrow) are visible within the tumor (**F**). B is 40×, **C and D** are 100×, **E** is 200×, and **F** is 400×. (**G-I**) Immunohistochemistry: CD34 (**G**) and STAT6 (**H**) are diffusely positive, and Ki-67 shows approximately 5% positivity in hotspot areas (**I**).

Table 2. The differential diagnosis of SFTL, HCC, FNH and AML.

Characteristics	SFTL	HCC	FNH	AML
Pathology	The tumor consists of irregularly arranged (fascicular) spindle or ovoid cells with oval nuclei and scant cytoplasm. Collagen-rich stroma and abundant staghorn (branching) thin-walled vessels (hemangiopericytoma-like vascular pattern) are present. Gene fusion, particularly the characteristic NAB2–STAT6 fusion, serves as a defining molecular feature of SFT	Exhibits structural and cytologic atypia (such as disorganized trabecular arrangement and increased nuclear-to-cytoplasmic ratio), and is often accompanied by stromal or vascular invasion.	Composed of a proliferative growth of morphologically normal hepatocytes but lacks normal portal tract development. Characteristic central fibrovascular scar and radiating fibrous septa are present, containing aberrant feeding arteries and their branches. Bile ductular proliferation is typically seen at the edges of the fibrous septa	It is primarily composed of 3 tissue components mixed in varying proportions: smooth muscle cells, adipose tissue, and blood vessels, with some cases containing hematopoietic tissue. Among these, smooth muscle cells (often epithelioid, with clear or eosinophilic cytoplasm) are the only specific diagnostic component, while the abnormal blood vessels are typically tortuous and thick-walled

Indexed in: [PMC] [PubMed] [Emerging Sources Citation Index (ESCI)] [Web of Science by Clarivate]

Table 2 continued. The differential diagnosis of SFTL, HCC, FNH and AML.

Characteristics	SFTL	HCC	FNH	AML
Epidemiologic features	Rare mesenchymal tumor; wide age range (median, 57 y); affects men and women	Adults, more common in men (60-70 y)	Adults, more common in women (30-50 y)	Adults, more common in women (50-60 y)
Clinical history	Mostly asymptomatic (incidental); large mass → abdominal discomfort, pain, weight loss, fatigue; rare Doege-Potter syndrome (IGF-II); 10-20% malignant potential	Chronic liver disease (HBV, HCV, alcoholic, NAFLD) in most cases; cirrhosis in vast majority	Normal/near-normal liver; asymptomatic (incidental); rare bleeding/rupture	Most asymptomatic (incidental); large lesions → discomfort, mild fever; sporadic or with tuberous sclerosis
Laboratory examination	Tumor markers negative/ normal; diagnosis: histology + IHC (CD34+, STAT6+, Vimentin+) + NAB2-STAT6 fusion	Frequently elevated serum AFP; linked to increased mortality and recurrence	Tumor markers (AFP, etc.) typically unremarkable	LFTs and tumor markers (AFP, CEA, CA19-9) usually normal/negative
US	Well-defined heterogeneous mass, hypo- or mildly hyperechoic; rare calcification; color Doppler: often no obvious internal or peripheral flow	Solid nodules on US; combined with AFP for high-risk monitoring	Often nearly isoechoic to normal liver (subtle differences); color/power Doppler: central feeding artery with characteristic "spoke-wheel" branches	Heterogeneous hyperechoic nodule (fat content) with shadowing/ refraction artifacts; may mimic hemangioma
CEUS	Intrinsic and extensive intratumoral small-vessel proliferation, arterial phase hyperenhancement; arterial phase: peripheral/ internal hyperenhancement, rapid centripetal filling; possible wash-out (hypoenhancement) on portal/delayed phases, possible central defect; mimic HCC	Disorganized external feeders; arterial non-rim hyperenhancement with subsequent washout	Central scar and spoke-wheel enhancement; portal/delayed phases: mild hyperenhancement or isoenhancement	Heterogeneous enhancement and irregular vascular morphology; arterial early: hyperenhancement, persists to portal/late phases; Approximately 25% may exhibit wash-out
CT	Plain scan: heterogeneous low density (solid soft tissue; necrotic/cystic areas lower); rare calcification and hemorrhage; after contrast: arterial phase marked heterogeneous enhancement; portal/delayed phases: persistent/progressive enhancement ("fast-in slow-out")	Early arterial marked hyperenhancement, delayed washout; may have peripheral enhancing pseudocapsule	Plain scan: iso- or slightly hypodense; arterial: homogeneous arterial phase hyperenhancement; central scar: hypo- in arterial/portal, hyper- in delayed (2-5 min)	Plain scan: heterogeneous low density, macroscopic fat (-100 to -10 HU); arterial: soft tissue markedly enhances; portal phase: persistent in most (some washout); common internal vessels and early draining veins

Indexed in: [PMC] [PubMed] [Emerging Sources Citation Index (ESCI)] [Web of Science by Clarivate]

Table 2 continued. The differential diagnosis of SFTL, HCC, FNH and AML.

Characteristics	SFTL	HCC	FNH	AML
MRI	T1: intermediate/low; T2: mixed high/low (low = fibrous/collagen), flow voids from vessels; Post-contrast: arterial heterogeneous; delayed progressive enhancement (fibrous)	Arterial enhancement + delayed washout; coating appearance; With hepatobiliary contrast, most HCCs are hypointense on HPB	T1 iso-/slightly hypointense; T2 slightly hyperintense ("invisible nodule"); arterial marked enhancement; central scar (T2 hyper/ T1 hypo) enhances delayed; hepatobiliary contrast: nearly uniform HBP hyperintensity (characteristic)	T2 heterogeneous hyperintense; T1 variable; in/opposed-phase: fat signal drop; Arterial hyperenhancement; possible washout on venous/delayed; HBP: hypointense

SFTL, solitary fibrous tumor of the liver; HCC, hepatocellular carcinoma; FNH, focal nodular hyperplasia; AML, angiomyolipoma; AFP, alpha-fetoprotein; HVB, hepatitis virus B; HVC, hepatitis virus C; CT, computed tomography; MRI, magnetic resonance imaging; NAFLD, nonalcoholic fatty liver disease; HPB, hepatobiliary phase; LFT, liver function tests; IHC, immunohistochemistry.

differentiating SFTL. For tumors in challenging locations adjacent to the portal vein, TACE can serve as an effective bridge to surgery by reducing tumor volume and facilitating subsequent resection. However, this report is limited by its single-case design, disease rarity, and short follow-up. Further studies with larger cohorts and longer follow-up are warranted to validate these findings and optimize clinical management of SFTL.

Department and Institution Where Work Was Done

Department of Ultrasound, the Third Affiliated Hospital of Sun Yat-Sen University, Guangzhou, Guangdong, PR China

Patient Consent

Written informed consent was obtained from the patient for the publication of this case report and related imaging data. The patient was fully informed of the study purpose, content, and data usage and agreed to participate voluntarily.

Declaration of Figures' Authenticity

All figures submitted have been created by the authors who confirm that the images are original with no duplication and have not been previously published in whole or in part.

References:

1. Wei P, Lo C, Gao J, et al. Systemic metastasis in malignant solitary fibrous tumor of the liver: Two case reports and literature review. Front Oncol. 2024;14:1418547
2. Badawy M, Nada A, Crim J, et al. Solitary fibrous tumors: Clinical and imaging features from head to toe. Eur J Radiol. 2022;146:110053
3. Rouy M, Guilbaud T, Birnbaum DJ. Liver solitary fibrous tumor: A rare incidentaloma. J Gastrointest Surg. 2021;25(3):852-53
4. Lu J. Contrast-enhanced ultrasound imaging features of solitary fibrous tumor in the liver: A case report. Asian J Surg. 2024;47(9):4026-27
5. Fuksbrumer MS, Klimstra D, Panicek DM. Solitary fibrous tumor of the liver: Imaging findings. Am J Roentgenol. 2000;175(6):1683-87
6. Salles-Silva E, de Castro PL, Ambrozino LC, et al. Rare benign liver tumors: Current insights and imaging challenges. Semin Ultrasound CT MR. 2025;46(3):154-60
7. Errico C, Pierre J, Pezet S, et al. Ultrafast ultrasound localization microscopy for deep super-resolution vascular imaging. Nature. 2015;527(7579):499-502
8. Réaux-Le-Goazigo A, Beliard B, Delay L, et al. Ultrasound localization microscopy and functional ultrasound imaging reveal atypical features of the trigeminal ganglion vasculature. Commun Biol. 2022;5(1): 330.
9. Li J, Wei C, Ying T, et al. Differentiation of benign and malignant breast lesions by ultrasound localization microscopy. Insights Imaging. 2025;16(1):128
10. Zhang W, Huang C, Yin T, et al. Ultrasensitive US microvessel imaging of hepatic microcirculation in the cirrhotic rat liver. Radiology. 2023;307(1):e220739
11. Ren C, D'Amato G, Hornicek FJ, et al. Advances in the molecular biology of the solitary fibrous tumor and potential impact on clinical applications. Cancer Metastasis Rev. 2024;43(4):1337-52
12. Nam HC, Sung PS, Jung ES, Yoon SK. Solitary fibrous tumor of the liver mimicking malignancy. Korean J Intern Med. 2020;35(3):734-35
13. Korkolis DP, Apostolaki K, Aggeli C, et al. Solitary fibrous tumor of the liver expressing CD34 and vimentin: A case report. World J Gastroenterol. 2008;14(40):6261-64
14. Chowdhury Z, Mishrikotkar S, Nehra P, et al. Exploring solitary fibrous tumors at a tertiary cancer center: Clinicopathological and immunomorphologic profile. Cureus. 2024;16(3):e56899
15. Vogel A, Meyer T, Sapisochin G, et al. Hepatocellular carcinoma. Lancet. 2022;400(10360):1345-62
16. Seow J, McGill M, Wang W, et al. Imaging hepatic angiomyolipomas: Key features and avoiding errors. Clin Radiol. 2020;75(2):88-99
17. LeGout JD, Bolan CW, Bowman AW, et al. Focal nodular hyperplasia and focal nodular hyperplasia-like lesions. Radiographics. 2022;42(4):1043-61
18. Petrolla AA, Xin W. Hepatic angiomyolipoma. Arch Pathol Lab Med. 2008;132(10):1679-82
19. Dong Y, Wang WP, Safai Zadeh E, et al. Comments and illustrations of the WFUMB CEUS liver guidelines: Rare benign focal liver lesion, part I. Med Ultrason. 2024;26(1):50-62

Indexed in: [PMC] [PubMed] [Emerging Sources Citation Index (ESCI)] [Web of Science by Clarivate]

20. Möller K, Tscheu T, De Molo C, et al. Comments and illustrations of the WFUMB CEUS liver guidelines: Rare congenital vascular pathology. Med Ultrason. 2022;24(4):461-72
21. Wang WL, Gokgoz N, Samman B, et al. RNA expression profiling reveals PRAME, a potential immunotherapy target, is frequently expressed in solitary fibrous tumors. Mod Pathol. 2021;34(5):951-60
22. Kacała A, Dorochowicz M, Matus I, et al. Hepatic hemangioma: Review of imaging and therapeutic strategies. Medicina (Kaunas). 2024;60(3):449
23. Dong ZR, Xia YN, Zhao YY, et al. Hepatic metastatic paraganglioma 12 years after retroperitoneal paraganglioma resection: A case report. BMC Gastroenterol. 2019;19(1):142

Indexed in: [PMC] [PubMed] [Emerging Sources Citation Index (ESCI)] [Web of Science by Clarivate]